Elliptic- and hyperbolic-function solutions of the nonlocal reverse-time and reverse-space-time nonlinear Schrödinger equations

Bo-Wen Li[1], Tao Xu[1,*], Tian-Li Zhang[1], Li-Cong An[1], and Yang Chen[1]

1. College of Science, China University of Petroleum, Beijing 102249, China

Abstract

In this paper, we obtain the stationary elliptic- and hyperbolic-function solutions of the nonlocal reverse-time and reverse-space-time nonlinear Schrödinger (NLS) equations based on their connection with the standard Weierstrass elliptic equation. The reverse-time NLS equation possesses the bounded dn-, cn-, sn-, sech-, and $\tanh$-function solutions. Of special interest, the $\tanh$-function solution can display both the dark- and antidark-soliton profiles. The reverse-space-time NLS equation admits the general Jacobian elliptic-function solutions (which are exponentially growing at one infinity or display the periodical oscillation in x), the bounded dn- and cn-function solutions, as well as the K-shifted dn- and sn-function solutions. At the degeneration, the hyperbolic-function solutions may exhibit an exponential growth behavior at one infinity, or show the gray- and bright-soliton profiles.

Keywords: Nonlocal nonlinear Schrödinger equation; Jacobian elliptic-function solutions; Hyperbolic-function solutions

*Corresponding author, e-mail: xutao@cup.edu.cn

1 Introduction

In the past several decades, a large number of integrable nonlinear partial differential equations (NPDEs) have been discovered and most of them are the local models [1]. As a prototypical local model, the nonlinear Schrödinger (NLS) equation [2]

$$iq_t(x,t) + q_{xx}(x,t) + \sigma q(x,t)q^*(x,t)q(x,t) = 0, \tag{1}$$

has arisen in various physical contexts to describe the evolution of weakly, quasi-monochromatic wave trains in the cubic nonlinear media [3], where the asterisk denotes complex conjugation, q is a complex-valued function of x and t, $\sigma = 1$ and -1 represent the focusing and defocusing types of nonlinearity, respectively. In 2013, Ablowitz and Musslimani [4] proposed the nonlocal reverse-space nonlinear Schrödinger (RSNLS) equation

$$iq_t(x,t) + q_{xx}(x,t) + \sigma q(x,t)q^*(-x,t)q(x,t) = 0. \tag{2}$$

Similar to the NLS equation, Eq. (2) is integrable in the sense that it has the Lax pair and an infinite number of conservation laws, and its initial-value problem can be solved by the inverse scattering transform (IST) [4]. The difference between such two equations lies in that the solution dynamics of Eq. (2) is non-locally dependent on the values of q at both the positions x and $-x$. As a new and simple integrable model, Eq. (2) was actively studied from different mathematical aspects, as seen in Refs. [5–11]. Meanwhile, wide classes of explicit solutions were obtained for both $\sigma = 1$ and $\sigma = -1$ cases by some analytical methods [4–6, 12–28]. For example, it was shown that Eq. (2) with $\sigma = -1$ admits the exponential, rational, exponential-and-rational solutions, which can display a rich variety of elastic soliton interactions on the nonzero background [6, 14–19].

Apart from Eq. (2), Ablowitz and Musslimani [29] also proposed the nonlocal reverse-time NLS (RTNLS) equation

$$iq_t(x,t) + q_{xx}(x,t) + \sigma q(x,t)q(x,-t)q(x,t) = 0, \tag{3}$$

and the nonlocal reverse-space-time NLS (RSTNLS) equation

$$iq_t(x,t) + q_{xx}(x,t) + \sigma q(x,t)q(-x,-t)q(x,t) = 0. \tag{4}$$

Eqs. (3) and (4) can arise from the second member of the Ablowitz-Kaup-Newell-Segur hierarchy respectively with the nonlocal reverse-time and reverse-space-time reductions, and their initial-value problems are solvable by the IST and Riemann-Hilbert method [23, 29–31]. Similar to Eq. (2), both the two equations are invariant under the the joint transformations $x \to -x$, $t \to -t$ and complex conjugation [29, 30]. It was shown that the solutions of Eqs. (3) and (4) in general exhibit the repeatedly-collapsing behavior, but they can still remain bounded or nonsingular for a certain range of parameter values [9]. For example, via the Darboux transformation Refs. [32, 33] revealed that Eq. (3) admits the nonsingular bright-soliton, dark-soliton, antidark-soliton, rogue-wave and breather solutions.

Following the pioneering work of Ablowitz and Musslimani, researchers soon realized that the nonlocal reverse-space, reverse-time and reverse-space-time reductions may exist in the known Ablowitz-Kaup-Newell-Segur [34], Kaup-Newell [35] and Wadati-Konno-Ichikawa [36] systems. As a result, a number of nonlocal integrable NPDEs were identified in $1+1$ and $1+2$ dimensions as well as in discrete settings [5, 29, 37–45]. At the same time, those integrable nonlocal equations have attracted certain interest in physics. For example, Eq. (2) is linked to an unconventional coupled Landau-Lifshitz system in magnetics through the gauge transformation [46], it can be derived as the quasi-monochromatic complex reductions of the cubic nonlinear Klein-Gordon, Korteweg-de Vries and water wave equations [47], and its stationary solutions can yield a wide class of complex, time-independent parity-time ($\mathcal{PT}$) symmetric potentials which may have applications in the $\mathcal{PT}$-symmetric quantum mechanics and optics [26]. Besides, several efforts have been made towards the physical realization of nonlocal coupling in unconventional settings, e.g., the nonlinear string where each particle is simultaneously coupled with nearest neighbors and its mirror particle [48].

As we know, the NLS equation possesses the stationary Jacobian elliptic-function and hyperbolic-function solutions [49, 50], where the former has the bounded periodical oscillation in x, while the latter displays the bright- or dark-soliton profile. Very recently, we constructed the stationary solutions of the RSNLS equation and revealed some unusual behaviors [26]: (i) The unbounded stationary solutions exponentially grow to infinity at $x \to \pm\infty$ but decay to zero at $x \to \mp\infty$; (ii) The bounded complex-amplitude solutions obey either the $\mathcal{PT}$- or anti-$\mathcal{PT}$ symmetry. In this paper, with the stationary-solution assumption, we will systematically search the Jacobian elliptic-function and hyperbolic-function solutions of Eqs. (3) and (4). First, we connect the RTNLS and RSTNLS equations with the standard Weierstrass elliptic (WE) equation, that is, Eq. (3) is directly reduced to the WE equation while Eq. (4) is connected with the WE equation based on the reduced equation and its x-symmetric counterpart. Then, we obtain that Eq. (3) has the dn-, cn- and sn-function solutions, whereas Eq. (4) admits the general Jacobian elliptic-function solutions (which are exponentially growing at one infinity or have the periodical oscillation in x), the bounded dn- and cn-function solutions, as well as the K-shifted dn- and sn-function solutions. Also, we derive the hyperbolic-function solutions which are degenerated from those Jacobian elliptic-function solutions. Specially, we find that the tanh-function solution of Eq. (3) can exhibit both the dark- and antidark-soliton profiles, and the hyperbolic-function solutions of Eq. (4) may exhibit an exponential growth at one infinity or show the gray- and bright-soliton profiles. Our results indicate the difference of solutions' behavior of Eqs. (3) and (4) compared with Eqs. (1) and (2).

2 Stationary solutions of the RTNLS equation

In this section, we construct the stationary solutions of Eq. (3) in the following form

$$q(x,t) = \phi(x) e^{i\,\mu t}, \tag{5}$$

where $\phi(x)$ represents the amplitude, μ is a real constant. Substituting the assumption (5) into Eq. (3) yields

$$\frac{\mathrm{d}^2\phi(x)}{\mathrm{d}x^2} - \mu\phi(x) + \sigma\phi^3(x) = 0. \tag{6}$$

Then, we multiply Eq. (6) by $2\frac{\mathrm{d}\phi(x)}{\mathrm{d}x}$ and integrate the resulting equation with respect to x, giving

$$\Big(\frac{\mathrm{d}\phi(x)}{\mathrm{d}x}\Big)^2 - \mu\phi^2(x) + \frac{1}{2}\sigma\phi^4(x) = C_0, \tag{7}$$

where C_0 is an integral constant. Through the transformation

$$\phi^2(x) = \frac{2\mu}{3\sigma} - \frac{2}{\sigma} w(x), \tag{8}$$

Eq. (7) becomes the standard WE equation

$$\Big(\frac{\mathrm{d}w(x)}{\mathrm{d}x}\Big)^2 = 4w^3(x) - g_2 w(x) - g_3, \tag{9}$$

where g_2 and g_3 are given by

$$g_2 = \frac{4}{3}\mu^2 + 2\sigma C_0, \quad g_3 = -\Big(\frac{8}{27}\mu^3 + \frac{2}{3}\sigma\mu C_0\Big). \tag{10}$$

As we know, Eq. (9) admits the following Jacobian elliptic-function solution [51]:

$$w(x) = r_3 + (r_2 - r_3)\mathrm{sn}^2(\sqrt{r_1 - r_3}\, x + x_0, m) \quad \left(m = \frac{r_2 - r_3}{r_1 - r_3}\right), \tag{11}$$

where x_0 is an arbitrary constant in $\mathbb{C}$, and r_i's ($1 \leq i \leq 3$, $r_1 + r_2 + r_3 = 0$) are the roots of the cubic equation

$$f(r) := 4r^3 - g_2 r - g_3 = 0. \tag{12}$$

In the following, we just consider that r_i's ($1 \leq i \leq 3$) are real numbers and satisfy the ordering relation $r_1 \geq r_2 \geq r_3$. At this moment, the coefficients g_2 and g_3 are real numbers, and the three roots of Eq. (12) can be given by $\frac{1}{3}\mu$, $-\frac{1}{6}\mu + \frac{1}{2}\sqrt{2\sigma C_0 + \mu^2}$ and $-\frac{1}{6}\mu - \frac{1}{2}\sqrt{2\sigma C_0 + \mu^2}$ with $C_0 \in \mathbb{R}$ and $\sigma C_0 \geq -\frac{\mu^2}{2}$. Then, based on Eq. (11), we obtain the Jacobian elliptic-function solutions ($r_1 > r_2 > r_3$) and hyperbolic-function solutions ($r_1 = r_2 > r_3$) of Eq. (3).

Case 1: Jacobian elliptic-function solutions

For the general case $r_1 > r_2 > r_3$, we have the following three families of Jacobian elliptic-function solutions:

(i) If $r_1 = \frac{1}{3}\mu$, $r_2 = -\frac{1}{6}\mu + \frac{1}{2}\sqrt{2\sigma C_0 + \mu^2}$, $r_3 = -\frac{1}{6}\mu - \frac{1}{2}\sqrt{2\sigma C_0 + \mu^2}$, we have the dn-function solution in the form

$$q = i^{\frac{1-\sigma}{2}} \sqrt{2}\, \alpha_1 \mathrm{dn}(\alpha_1 x + x_0, m_1) e^{i\mu t}, \tag{13}$$

where α_1 and m_1 are given by

$$\alpha_1 = \sqrt{\frac{\mu}{2 - m_1}}, \quad m_1 = \frac{2\sqrt{2\sigma C_0 + \mu^2}}{\mu + \sqrt{2\sigma C_0 + \mu^2}} \quad (-\mu^2 < 2\sigma C_0 < 0,\ \mu > 0). \tag{14}$$

(ii) If $r_1 = -\frac{1}{6}\mu + \frac{1}{2}\sqrt{2\sigma C_0 + \mu^2}$, $r_2 = \frac{1}{3}\mu$, $r_3 = -\frac{1}{6}\mu - \frac{1}{2}\sqrt{2\sigma C_0 + \mu^2}$, we have the cn-function solution in the form

$$q = i^{\frac{1-\sigma}{2}} \sqrt{2m_2}\, \alpha_2 \mathrm{cn}(\alpha_2 x + x_0, m_2) e^{i\mu t}, \tag{15}$$

where α_2 and m_2 are given by

$$\alpha_2 = \sqrt{\frac{\mu}{2m_2 - 1}}, \quad m_2 = \frac{\mu + \sqrt{2\sigma C_0 + \mu^2}}{2\sqrt{2\sigma C_0 + \mu^2}} \quad (\sigma C_0 > 0, \mu \in \mathbb{R}). \tag{16}$$

(iii) If $r_1 = -\frac{1}{6}\mu + \frac{1}{2}\sqrt{2\sigma C_0 + \mu^2}$, $r_2 = -\frac{1}{6}\mu - \frac{1}{2}\sqrt{2\sigma C_0 + \mu^2}$, $r_3 = \frac{1}{3}\mu$, we have the sn-function solution in the form

$$q = i^{\frac{1+\sigma}{2}}\sqrt{2m_3}\,\alpha_3 \mathrm{sn}(\alpha_3 x + x_0, m_3)e^{i\mu t}, \tag{17}$$

where α_3 and m_3 are given by

$$\alpha_3 = \sqrt{\frac{-\mu}{1+m_3}}, \quad m_3 = \frac{\mu + \sqrt{2\sigma C_0 + \mu^2}}{\mu - \sqrt{2\sigma C_0 + \mu^2}} \quad (-\mu^2 < 2\sigma C_0 < 0,\ \mu < 0). \tag{18}$$

One should note that since x_0 can be selected in $\mathbb{C}$, solutions (13), (15) and (17) possess in general the complex amplitudes, regardless of the sign σ. Particularly when $x_0 \in \mathbb{R}$, all the three solutions have the purely real or imaginary amplitudes (depending on σ) and they also solve the NLS equation (1). In fact, the general Jacobian elliptic-function solutions with complex amplitudes for Eq. (1) can be constructed in a different way (see the case $C_1 < 0$ in subsection 3.2.1).

In addition, the constant x_0 must be judiciously selected in avoid that the Jacobian elliptic-function solutions (13), (15) and (17) are non-singular. In the complex z-plane, $\mathrm{sn}(z, m)$ has simple poles which are congruent to iK' or to $2K + iK'$ (mod. $4K, 2iK'$), $\mathrm{cn}(z, m)$ has simple poles which are congruent to iK' or to $2K + iK'$ (mod. $4K, 2K + 2iK'$), and $\mathrm{dn}(z, m)$ has simple poles which are congruent to iK' or to $3iK'$ (mod. $2K, 4iK'$) [51], where K and K' are the complete elliptic integrals of the first kind

$$K = K(m) = \int_0^{\frac{\pi}{2}} \frac{dt}{\sqrt{1 - m\sin^2 t}}, \quad K' = K'(m) = K(1-m). \tag{19}$$

Therefore, it requires that $x_{0I} \neq (2n+1)K'$ $(n \in \mathbb{Z})$ with $x_{0I} = \mathrm{Im}(x_0)$ to ensure that solutions (13), (15) and (17) have no singularity for all $x \in (-\infty, \infty)$.

Case 2: Hyperbolic-function solutions

When particularly taking $r_1 = r_2 > r_3$, we have $m = 1$, so that the Jacobian elliptic functions degenerate to the hyperbolic functions. As a result, we obtain two families of hyperbolic-function solutions as follows:

(i) If $\frac{1}{3}\mu = -\frac{1}{6}\mu + \frac{1}{2}\sqrt{2\sigma C_0 + \mu^2} > -\frac{1}{6}\mu - \frac{1}{2}\sqrt{2\sigma C_0 + \mu^2}$, one immediately have $r_1 = r_2 = \frac{1}{3}\mu$, $r_3 = -\frac{2}{3}\mu$ $(\mu > 0)$, and $C_0 = 0$. Then, both solutions (13) and (15) become the sech-function form

$$q = i^{\frac{1-\sigma}{2}}\sqrt{2\mu}\,\mathrm{sech}(\sqrt{\mu}\,x + x_0)e^{i\mu t} \quad (\mu > 0). \tag{20}$$

(ii) If $-\frac{1}{6}\mu + \frac{1}{2}\sqrt{2\sigma C_0 + \mu^2} = -\frac{1}{6}\mu - \frac{1}{2}\sqrt{2\sigma C_0 + \mu^2} > \frac{1}{3}\mu$, one have $r_1 = r_2 = -\frac{1}{6}\mu$, $r_3 = \frac{1}{3}\mu$ $(\mu < 0)$, and $C_0 = -\frac{\sigma}{2}\mu^2$. Then, solution (17) becomes the $\tanh$-function form

$$q = i^{\frac{1+\sigma}{2}}\sqrt{-\mu}\,\tanh(\sqrt{-\mu/2}\,x + x_0)e^{i\mu t} \quad (\mu < 0). \tag{21}$$

Considering the analyticity of the sech and $\tanh$ functions in the complex z-plane, we know that solutions (20) and (21) are both nonsingular if and only if $x_{0I} \neq \frac{2n+1}{2}\pi$ $(n \in \mathbb{Z})$.

Different from the bright and dark-soliton solutions of Eq. (1), the profiles of solutions (20) and (21) may vary with the parameter x_{0I}. For solution (20), its intensity has just one maximum and thus it always displays the bright-soliton profile on the zero background, as seen in Fig. 1. The soliton amplitude can be given by $A = \sqrt{2\mu}\big|\sec(x_{0I})\big|$ $(\mu > 0)$, which shows that the amplitude increases in the interval $\left[n\pi, \frac{2n+1}{2}\pi\right)$ but decreases in the interval $\left(\frac{2n+1}{2}\pi, (n+1)\pi\right]$ with the increment of x_{0I}. Likewise, the intensity of solution (21) has one extremum whose value is $-\mu\tan^2(x_{0I})$. By calculating the difference between the extremum value and background amplitude, one can find that solution (21) represents the dark soliton if $x_{0I} \in \left[\frac{4n-1}{4}\pi, \frac{4n+1}{4}\pi\right]$ (see Fig. 2) or antidark soliton if $x_{0I} \in \left(\frac{2n-1}{2}\pi, \frac{4n-1}{4}\pi\right) \cup \left(\frac{4n+1}{4}\pi, \frac{2n+1}{2}\pi\right)$ on the nonzero background (see Fig. 3).

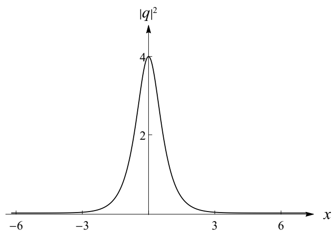

Figure 1: Soliton profile via solution (20) at $\mu = 1$ with $x_0 = \frac{3}{4}\pi i$.

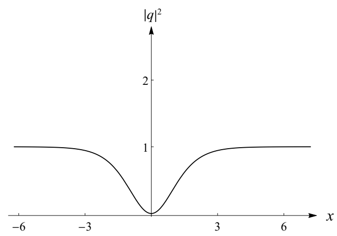

Figure 2: Soliton profile via solution (21) at $\mu = -1$ with $x_0 = 0$.

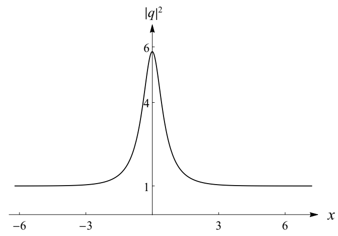

Figure 3: Soliton profile via solution (21) at $\mu = -1$ with $x_0 = \frac{3}{8}\pi i$.

3 Stationary solutions of the RSTNLS equation

3.1 Connection of Eq. (4) with the elliptic equation

Likewise, using the assumption (5), Eq. (4) can be reduced to

$$\frac{\mathrm{d}^2\phi(x)}{\mathrm{d}x^2} - \mu\phi(x) + \sigma\phi^2(x)\phi(-x) = 0. \tag{22}$$

Here, because of the nonlinear term $\sigma\phi^2(x)\phi(-x)$, Eq. (22) cannot be directly converted into the elliptic equation like Eq. (6). However, we note that $\phi(-x)$ also satisfies Eq. (22), that is,

$$\frac{\mathrm{d}^2\phi(-x)}{\mathrm{d}x^2} - \mu\phi(-x) + \sigma\phi^2(-x)\phi(x) = 0. \tag{23}$$

In the following, we use Eqs. (22) and (23) together to establish the relationship of Eq. (4) with the elliptic equation.

On one side, we multiply Eqs. (22) and (23) respectively by $2\frac{\mathrm{d}\phi(-x)}{\mathrm{d}x}$ and $2\frac{\mathrm{d}\phi(x)}{\mathrm{d}x}$, and integrate their sum with respect to x, obtaining that

$$2\frac{\mathrm{d}\phi(x)}{\mathrm{d}x}\cdot\frac{\mathrm{d}\phi(-x)}{\mathrm{d}x} - 2\mu\phi(x)\phi(-x) + \sigma\phi^2(x)\phi^2(-x) = C_0, \tag{24}$$

where C_0 is an integral constant. Again, multiplying Eqs. (22) and (23) respectively by $\phi(-x)$ and $\phi(x)$ and adding them to Eq. (24) gives rise to

$$\frac{\mathrm{d}^2 w(x)}{\mathrm{d}x^2} - 4\mu w(x) + 3\sigma w^2(x) = C_0, \quad w(x) = \phi(x)\phi(-x). \tag{25}$$

Further, by multiplying Eq. (25) by $\frac{\mathrm{d}w(x)}{\mathrm{d}x}$ and integrating the resultant equation once with respect to x, we arrive at the elliptic equation for $w(x)$:

$$\left(\frac{\mathrm{d}w(x)}{\mathrm{d}x}\right)^2 - 4\mu w^2(x) + 2\sigma w^3(x) = 2C_0 w(x) + C_1, \tag{26}$$

where C_1 is also an integral constant, and $w(x)$ obeys the relation $w(x) = w(-x)$.

On the other side, we multiply Eqs. (22) and (23) respectively by $\phi(-x)$ and $\phi(x)$, and then integrate their subtraction with respect to x, yielding

$$\phi(x)\frac{\mathrm{d}\phi(-x)}{\mathrm{d}x} - \phi(-x)\frac{\mathrm{d}\phi(x)}{\mathrm{d}x} = C_2, \tag{27}$$

where C_2 is an integral constant. Divided by $\phi^2(x)$ or $\phi^2(-x)$, Eq. (27) becomes

$$\frac{\mathrm{d}}{\mathrm{d}x}\left(\frac{w(x)}{\phi^2(x)}\right) = \frac{C_2}{w(x)} \cdot \frac{w(x)}{\phi^2(x)}, \text{ or } \frac{\mathrm{d}}{\mathrm{d}x}\left(\frac{w(x)}{\phi^2(-x)}\right) = \frac{-C_2}{w(x)} \cdot \frac{w(x)}{\phi^2(-x)}. \tag{28}$$

Note that Eq. (28) can be regarded as a linear differential equation with respect to $w(x)/\phi^2(x)$ or $w(x)/\phi^2(-x)$ once $w(x)$ is solved from Eq. (26) and satisfies the symmetric relation $w(x) = w(-x)$. Thus, we have

$$\phi^2(x) = \rho_1^2 w(x) e^{-\int_{x_0}^{x} \frac{C_2}{w(s)} ds}, \quad \phi^2(-x) = \rho_2^2 w(x) e^{\int_{x_0}^{x} \frac{C_2}{w(s)} ds}. \tag{29}$$

In view of $\phi^2(x)|_{x\to -x} = \phi^2(-x)$ and $\phi^2(x)\phi^2(-x) = w^2(x)$, we obtain that ρ_1 and ρ_2 obey the relation

$$\rho_1 = \frac{1}{\rho_2} = e^{-\frac{1}{4}\int_{-x_0}^{x_0} \frac{C_2}{w(s)} ds}. \tag{30}$$

Here, we still need to check if $\phi(x)$ and $\phi(-x)$ in Eq. (29) satisfy Eq. (22). First, the second-order derivative of $\phi(x)$ is given by

$$\frac{\mathrm{d}^2\phi(x)}{\mathrm{d}x^2} = \frac{\phi(x)}{4w^2(x)}\left[C_2^2 - \left(\frac{\mathrm{d}w(x)}{\mathrm{d}x}\right)^2\right] + \frac{\phi(x)}{2w(x)}\frac{\mathrm{d}^2 w(x)}{\mathrm{d}x^2}. \tag{31}$$

Then, substituting (31) into (22) and removing $\left(\frac{\mathrm{d}w(x)}{\mathrm{d}x}\right)^2$ and $\frac{\mathrm{d}^2 w(x)}{\mathrm{d}x^2}$ via Eqs. (25) and (26), the resulting equation reads

$$\frac{\mathrm{d}^2\phi(x)}{\mathrm{d}x^2} - \mu\phi(x) + \sigma\phi^2(x)\phi(-x) = \frac{C_2^2 - C_1}{4w^2(x)}\phi(x), \tag{32}$$

where $w(x) = \phi(x)\phi(-x)$ has been used for simplification. Clearly, Eq. (32) shows that $\phi(x)$ and $\phi(-x)$ given in Eq. (29) obey Eq. (22) if and only if $C_1 = C_2^2$. Therefore, we finally reach the following result:

Proposition 3.1 *Assume that $w(x)$ is an solution of Eq. (26) with $w(x) = w(-x)$, and $w^{\frac{1}{2}}(x)$ is also a smooth even function. Then, we have a pair of solutions for Eq. (22):*

$$\phi(x) = \rho_1 w^{\frac{1}{2}}(x) e^{-\frac{1}{2}\int_{x_0}^{x} \frac{C_2}{w(s)} ds}, \quad \phi(-x) = \frac{1}{\rho_1} w^{\frac{1}{2}}(x) e^{\frac{1}{2}\int_{x_0}^{x} \frac{C_2}{w(s)} ds}, \tag{33}$$

where $\rho_1 = e^{-\frac{1}{4}\int_{-x_0}^{x_0} \frac{C_2}{w(s)} ds}$ and $C_2 = C_1^{\frac{1}{2}}$. If $C_2 \neq 0$, $\phi(x)$ and $\phi(-x)$ are mutually independent, whereas they coalesce into one solution at $C_2 = 0$.

Remark 1. It should be noted that even if $w(x)$ is a real-valued, even-symmetric solution of Eq. (26), Eq. (33) may not yield the *smooth* functions for $\phi(x)$ and $\phi(-x)$. In fact, an obvious *necessary* condition ensuring the smoothness of $\phi(x)$ and $\phi(-x)$ is

$$w(x) \geq 0 \text{ or } w(x) \leq 0 \text{ for all } x \in \mathbb{R}. \tag{34}$$

This is because the sign indefiniteness of $w(x)$ may cause $\phi(x)$ and $\phi(-x)$ non-smooth at points where the sign changes. However, there are still some exceptions even if condition (34) holds. For example, with $C_0 = -\sigma\mu^2$ and $C_1 = 0$, solving Eq. (26) gives the following solution:

$$w(x) = \sigma\mu \tanh^2\left(\sqrt{\frac{-\mu}{2}}\, x\right) \quad (\mu < 0). \tag{35}$$

One can check that Eq. (35) satisfies condition (34) for both $\sigma = \pm 1$ cases, but its square root cannot yield the smooth even function.

3.2 Jacobian elliptic-function and hyperbolic-function solutions

Through the transformation

$$w(x) = \frac{2\mu}{3\sigma} - \frac{2}{\sigma} w_1(x), \tag{36}$$

one can also transform Eq. (26) into the standard WE equation:

$$\left(\frac{\mathrm{d}w_1(x)}{\mathrm{d}x}\right)^2 = 4w_1^3(x) - g_2 w_1(x) - g_3, \tag{37}$$

where g_2 and g_3 are given by

$$g_2 = \sigma C_0 + \frac{4}{3}\mu^2, \quad g_3 = -\left(\frac{1}{3}\sigma\mu C_0 + \frac{1}{4}C_1 + \frac{8}{27}\mu^3\right). \tag{38}$$

Thus, we give the Jacobian elliptic-function solution of Eq. (4) as follows:

$$w(x) = 2\sigma\left[\frac{\mu}{3} - r_3 - (r_2 - r_3)\mathrm{sn}^2(\sqrt{r_1 - r_3}\, x, m)\right] \quad \left(m = \frac{r_2 - r_3}{r_1 - r_3}\right). \tag{39}$$

Here, compared with solution (11), we ignore the constant x_0 because the symmetric condition $w(x) = w(-x)$ restricts that x_0 is no longer an arbitrary constant. In section 3.2.2, we will discuss the possible nonzero choice of x_0.

Again, we consider that r_i's ($1 \leq i \leq 3$) are real numbers and obey the ordering relation $r_1 \geq r_2 \geq r_3$. Thus, the coefficients g_2 and g_3 must be real numbers, which means that C_0 and C_1 are two real constants. Besides, the modular discriminant should satisfy

$$\Delta := g_2^3 - 27g_3^2 = -\frac{27}{16}C_1^2 - \left(\frac{9}{2}\sigma\mu C_0 + 4\mu^3\right)C_1 + C_0^2(\mu^2 + \sigma C_0) \geq 0, \tag{40}$$

which holds if and only if C_0, C_1 and μ obey

$$\begin{cases} \Omega := \sqrt{(3\sigma C_0 + 4\mu^2)^3} \geq 0, \\ -\frac{4}{27}\left(9\sigma\mu C_0 + 8\mu^3 + \Omega\right) \leq C_1 \leq -\frac{4}{27}\left(9\sigma\mu C_0 + 8\mu^3 - \Omega\right). \end{cases} \tag{41}$$

In the following, we present all the possible Jacobian elliptic-function solutions $(r_1 > r_2 > r_3)$ and hyperbolic-function solutions $(r_1 = r_2 > r_3)$ of Eq. (4) with condition (41).

3.2.1 Jacobian elliptic-function solutions

Based on Eqs. (33) and (39), we have the Jacobian elliptic-function solutions of Eq. (4) in the form

$$q=\sqrt{\sigma\Big[\frac{2\mu}{3}-2r_3-2(r_2-r_3)\mathrm{sn}^2(\sqrt{r_1-r_3}\,x,m)\Big]}\,e^{\frac{-3\sigma C_2\Pi\left(\frac{3(r_2-r_3)}{\mu-3r_3};\Phi(x),m\right)}{4(\mu-3r_3)\sqrt{r_1-r_3}}+i\,\mu t}, \tag{42}$$

where $m=\frac{r_2-r_3}{r_1-r_3}$, $\Phi(x)=\mathrm{am}\,(\sqrt{r_1-r_3}\,x,m)$ is the Jacobian amplitude, Π is the incomplete elliptic integral of the third kind. According to remark 1, $w(x)$ in Eq. (39) must be sign definite for all $x\in\mathbb{R}$ to ensure the smoothness of solution (42). Because $0\leq\mathrm{sn}^2(\sqrt{r_1-r_3}\,x,m)\leq 1$, it requires that $r_2\leq\frac{1}{3}\mu$ or $r_3\geq\frac{1}{3}\mu$. Meanwhile, we notice that

$$\begin{cases} f(r)<0, & r\in(-\infty,r_3)\cup(r_2,r_1),\\ f(r)>0, & r\in(r_3,r_2)\cup(r_1,\infty),\\ f(r)=\frac{C_1}{4}, & r=\frac{1}{3}\mu\ (C_1=C_2^2), \end{cases} \tag{43}$$

which shows that the distribution of three roots r_i's is dependent on μ and C_1. Next, we judge the range of μ when C_1 is given and discuss the properties of the Jacobian elliptic-function solutions in Eq. (42).

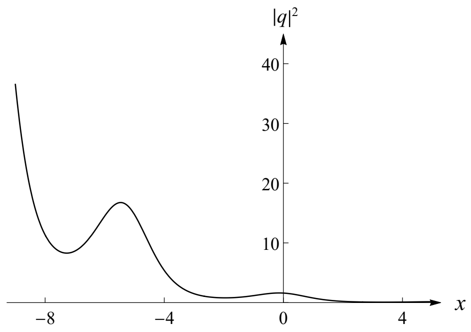

Figure 4: Intensity profile of solution (42) with $\sigma=1$, $C_0=-\frac{2}{3}$, $C_1=\frac{2}{27}$, $C_2=\sqrt{\frac{2}{27}}$ and $\mu=1$.

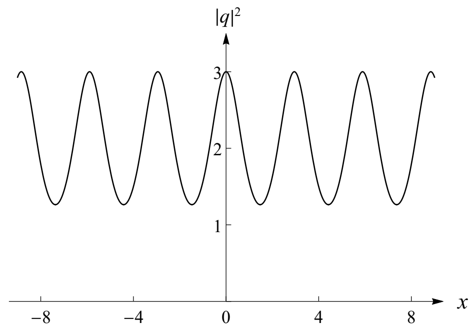

Figure 5: Intensity profile of solution (42) with $\sigma=1$, $C_0=-\frac{8}{3}$, $C_1=-2$, $C_2=\sqrt{2}i$ and $\mu=2$.

Case 1: $C_1>0$

In this case, $f(\frac{1}{3}\mu)>0$ implies that $\frac{1}{3}\mu\in(r_3,r_2)\cup(r_1,\infty)$. Meanwhile, considering the sign definiteness of $w(x)$, we know that $\frac{1}{3}\mu>r_1$. Therefore, we have $w(x)>0$ for $\sigma=1$ and $w(x)<0$ for $\sigma=-1$. In addition, $C_2^2=C_1>0$ indicates that C_2 is a real constant. Thus, the intensity of $q(x,t)$ will grow to ∞ as $\sigma\,\mathrm{sgn}(C_2)x\to-\infty$ but decay to 0 as $\sigma\,\mathrm{sgn}(C_2)x\to\infty$ in an exponential-and-periodical manner. For example, with $\sigma=1$, $C_0=-\frac{2}{3}$, $C_1=\frac{2}{27}$ and $\mu=1$, we obtain $r_1=\frac{\sqrt{21}-1}{12}$, $r_2=\frac{1}{6}$ and $r_3=-\frac{\sqrt{21}+1}{12}$. The intensity profile of $q(x,t)$ is shown in Fig. 4.

Case 2: $C_1<0$

In this case, because $f(\frac{1}{3}\mu)<0$, we know that $\frac{1}{3}\mu\in(-\infty,r_3)\cup(r_2,r_1)$. If $\frac{1}{3}\mu<r_3$, $w(x)<0$ for $\sigma=1$ and $w(x)>0$ for $\sigma=-1$; whereas if $r_2<\frac{1}{3}\mu<r_1$, $w(x)>0$ for $\sigma=1$ and $w(x)<0$ for $\sigma=-1$. In view that C_2 is a pure imaginary number ($C_2^2=C_1<0$), the solution is bounded for all $x\in\mathbb{R}$. The intensity of $q(x,t)$ exhibits the periodical oscillation behavior in x but do not drop to zero at its all minima. For example, when $\sigma = 1$, $C_0 = -\frac{8}{3}$, $C_1 = -2$ and $\mu = 2$, we have $r_1 = \frac{5+\sqrt{21}}{12}$, $r_2 = \frac{5-\sqrt{21}}{12}$ and $r_3 = -\frac{5}{6}$. The intensity profile of $q(x,t)$ is displayed in Fig. 5.

Case 3: $C_1 = 0$

For this case, the three roots of $f(r)$ are given by $\frac{1}{3}\mu$, $-\frac{1}{6}\mu + \frac{1}{2}\sqrt{\sigma C_0 + \mu^2}$ and $-\frac{1}{6}\mu - \frac{1}{2}\sqrt{\sigma C_0 + \mu^2}$. According to the ordering of the three roots, we obtain two families of bounded Jacobian elliptic-function solutions as follows:

(i) If $r_1 = \frac{1}{3}\mu$, $r_2 = -\frac{1}{6}\mu + \frac{1}{2}\sqrt{\sigma C_0 + \mu^2}$ and $r_3 = -\frac{1}{6}\mu - \frac{1}{2}\sqrt{\sigma C_0 + \mu^2}$, Eq. (39) gives rise to

$$w(x) = 2\,\sigma\,\alpha_1^2\,\mathrm{dn}^2(\alpha_1 x, m_1), \tag{44}$$

where α_1 and m_1 are given by

$$\alpha_1 = \sqrt{\frac{\mu}{2 - m_1}}, \quad m_1 = \frac{2\sqrt{\sigma C_0 + \mu^2}}{\mu + \sqrt{\sigma C_0 + \mu^2}} \quad (-\mu^2 < \sigma C_0 < 0,\ \mu > 0). \tag{45}$$

Thus, we obtain the dn-function solution in the form

$$q = i^{\frac{1-\sigma}{2}}\sqrt{2}\,\alpha_1\,\mathrm{dn}(\alpha_1 x, m_1)e^{i\mu t}. \tag{46}$$

(ii) If $r_1 = -\frac{1}{6}\mu + \frac{1}{2}\sqrt{\sigma C_0 + \mu^2}$, $r_2 = \frac{1}{3}\mu$ and $r_3 = -\frac{1}{6}\mu - \frac{1}{2}\sqrt{\sigma C_0 + \mu^2}$, Eq. (39) gives rise to

$$w(x) = 2\,\sigma\,m_2\,\alpha_2^2\,\mathrm{cn}^2(\alpha_2 x, m_2), \tag{47}$$

where α_2 and m_2 are given by

$$\alpha_2 = \sqrt{\frac{\mu}{2m_2 - 1}}, \quad m_2 = \frac{\mu + \sqrt{\sigma C_0 + \mu^2}}{2\sqrt{\sigma C_0 + \mu^2}} \quad (\sigma C_0 > 0, \mu \in \mathbb{R}). \tag{48}$$

Thus, we obtain the cn-function solution in the form

$$q = i^{\frac{1-\sigma}{2}}\sqrt{2m_2}\,\alpha_2 \mathrm{cn}(\alpha_2 x, m_2)e^{i\mu t}. \tag{49}$$

For the third case $r_1 = -\frac{1}{6}\mu + \frac{1}{2}\sqrt{\sigma C_0 + \mu^2}$, $r_2 = -\frac{1}{6}\mu - \frac{1}{2}\sqrt{\sigma C_0 + \mu^2}$ and $r_3 = \frac{1}{3}\mu$, one can also obtain the sign-definite $w(x)$ as follows:

$$w(x) = -2\,\sigma\,m_3\,\alpha_3^2\,\mathrm{sn}^2(\alpha_3 x, m_3), \tag{50}$$

with

$$\alpha_3 = \sqrt{\frac{-\mu}{1 + m_3}}, \quad m_3 = \frac{\mu + \sqrt{\sigma C_0 + \mu^2}}{\mu - \sqrt{\sigma C_0 + \mu^2}} \quad (-\mu^2 < \sigma C_0 < 0,\ \mu < 0). \tag{51}$$

However, the square root of $w(x)$ in Eq. (50) yields no smooth even function, so that one cannot obtain the smooth $\phi(x)$ from Eq. (33).

3.2.2 K-shifted Jacobian elliptic-function solutions

For $w(x)$ in Eq. (39), we introduce the complex constant x_0 and impose

$$\mathrm{sn}^2(\sqrt{r_1-r_3}x+x_0,m)=\mathrm{sn}^2(-\sqrt{r_1-r_3}x+x_0,m), \tag{52}$$

to satisfy the relation $w(x)=w(-x)$. Based on the properties of the sn-function, condition (52) holds true if and only if $x_0=lK+i\,nK'(l,n\in\mathbb{Z})$, where K and K' are defined in Eq. (19). In order to avoid the singularity, we must take n as an even integer. Moreover, the periodicity of $\mathrm{sn}^2(x)$ implies that the only nonzero value of x_0 is K.

When $C_1\neq 0$, we make the shift $\sqrt{r_1-r_3}x\to\sqrt{r_1-r_3}x+K$ for $w(x)$ in Eq. (39), and then obtain the K-shifted Jacobian elliptic-function solutions as follows:

$$\begin{aligned} q^{(K)}=&\sqrt{2\sigma\Big[\frac{\mu}{3}-r_3-(r_2-r_3)\mathrm{sn}^2(\sqrt{r_1-r_3}\,x+K,m)\Big]}\\ &\times e^{-\frac{3\sigma C_2}{4}\left[\frac{3(r_2-r_1)}{(\mu-3r_1)(\mu-3r_2)\sqrt{r_1-r_3}}\Pi\left(\frac{m(\mu-3r_1)}{\mu-3r_2};\Phi(x),m\right)+\frac{x}{\mu-3r_1}\right]+i\,\mu t}, \end{aligned} \tag{53}$$

with $m=\frac{r_2-r_3}{r_1-r_3}$ and $\Phi(x)=\mathrm{am}\,(\sqrt{r_1-r_3}\,x,m)$. Since the sign of $w(x)$ does not change with the K-shift in x, thus it has no influence on the smoothness of $q^{(K)}$. Like the cases 1 and 2 in section 3.2.1, solution (53) possesses the similar dynamical properties: If $C_1>0$ and $\frac{1}{3}\mu\in(r_1,\infty)$, the intensity of $q^{(K)}$ grows to ∞ at one infinity but decays to 0 at the other infinity in an exponential-and-periodical manner; if $C_1<0$ and $\frac{1}{3}\mu\in(-\infty,r_3)\cup(r_2,r_1)$, the intensity of $q^{(K)}$ displays the periodical oscillation in x.

When $C_1=0$, we also make the shift $\alpha_i x\to\alpha_i x+K_i\,(1\le i\le 3)$ for $w(x)$ in Eqs. (44), (47) and (50), respectively. Then, from the following properties

$$\begin{aligned} \mathrm{dn}(\alpha_1x+K_1,m_1)&=\mathrm{dn}(-\alpha_1x+K_1,m_1),\\ \mathrm{cn}(\alpha_2x+K_2,m_2)&=-\mathrm{cn}(-\alpha_2x+K_2,m_2),\\ \mathrm{sn}(\alpha_3x+K_3,m_3)&=\mathrm{sn}(-\alpha_3x+K_3,m_3), \end{aligned} \tag{54}$$

we know that both $\mathrm{dn}(\alpha_1x+K_1,m_1)$ and $\mathrm{sn}(\alpha_3x+K_3,m_3)$ are even functions, whereas $\mathrm{cn}(\alpha_2x+K_2,m_2)$ is an odd function. That is, the K-shift changes the parity of the cn and sn functions, but has no change for the dn-function. Recall that $w^{\frac{1}{2}}(x)$ must be even symmetric to ensure that $q(x,t)$ is a smooth function. Therefore, associated with $w(x)$ in Eqs. (44) and (47), we obtain two families of shifted Jacobian elliptic-function solutions:

$$q^{(K_1)}=i^{\frac{1-\sigma}{2}}\sqrt{2}\,\alpha_1\,\mathrm{dn}(\alpha_1x+K_1,m_1)e^{i\mu t}\quad(\mu>0), \tag{55}$$

$$q^{(K_3)}=i^{\frac{1+\sigma}{2}}\sqrt{2m_3}\,\alpha_3\mathrm{sn}(\alpha_3x+K_3,m_3)e^{i\mu t}\quad(\mu<0), \tag{56}$$

where $\alpha_{1,3}$ and $m_{1,3}$ are defined in Eqs. (45) and (51).

3.2.3 Hyperbolic-function solutions

In this subsection, we consider the degenerate cases for all the Jacobian elliptic-function solutions in section 3.2.1 at $r_1=r_2>r_3$. In those cases, we can express C_0 and C_1 in terms of r_1:

$$C_0=\frac{4\sigma}{3}(9r_1^2-\mu^2),\quad C_1=\frac{16}{27}(\mu-3r_1)^2(\mu+6r_1). \tag{57}$$

As a result, $w(x)$ in Eq. (39) reduces to

$$w(x) = 2\sigma\Big[\frac{1}{3}\,\mu + 2r_1 - 3r_1\tanh^2(\sqrt{3r_1}\,x)\Big], \tag{58}$$

where r_3 has been removed by $r_3 = -2r_1$. To maintain the sign definiteness of $w(x)$, there are the following three cases:

Case 1: $0 < r_1 < \frac{1}{3}\mu$ $(\mu > 0)$

In this case, $w(x) > 0$ for all $x \in \mathbb{R}$ and C_1 is a positive real constant. Thus, we obtain the following unbounded hyperbolic-function solution:

$$q = \sqrt{w(x)}V(x)e^{-\sigma\sqrt{\frac{\mu+6r_1}{3}}x+i\mu t}, \tag{59}$$

with

$$V(x) = \left[\frac{1+3\sqrt{\frac{r_1}{\mu+6r_1}}\tanh(\sqrt{3r_1}x)}{1-3\sqrt{\frac{r_1}{\mu+6r_1}}\tanh(\sqrt{3r_1}x)}\right]^{\frac{\sigma}{2}}. \tag{60}$$

Note that $\mu + 6r_1 > 0$ and $V(x)$ is a bounded function since $-1 < \tanh(\sqrt{3r_1}x) < 1$ and $\sqrt{\frac{r_1}{\mu+6r_1}} < \frac{1}{3}$. Thus, the intensity of $q(x,t)$ will grow exponentially to ∞ as $\sigma x \to -\infty$ or decay exponentially to 0 as $\sigma x \to \infty$. For example, by taking $C_0 = -\frac{7}{192}$, $C_1 = \frac{5}{3456}$, $\mu = \frac{1}{4}$ and $\sigma = 1$ ($r_1 = \frac{1}{16}$), we illustrate the profile of solution (59) in Fig. 6.

Case 2: $r_1 < -\frac{1}{6}\mu$ $(\mu < 0)$

In this case, $w(x) < 0$ for all $x \in \mathbb{R}$ and C_1 is a negative real constant. Thus, we obtain the following bounded hyperbolic-function solution:

$$q = \sqrt{w(x)}V(x)e^{-i\sigma\sqrt{\frac{-\mu-6r_1}{3}}x+i\mu t}, \tag{61}$$

with

$$V(x) = \left[\frac{1+3i\sqrt{\frac{-r_1}{\mu+6r_1}}\tanh(\sqrt{3r_1}x)}{1-3i\sqrt{\frac{-r_1}{\mu+6r_1}}\tanh(\sqrt{3r_1}x)}\right]^{\frac{\sigma}{2}}. \tag{62}$$

Because $\mu + 6r_1 < 0$, we have $\big|V(x)e^{-i\sigma\sqrt{\frac{-\mu-6r_1}{3}}x}\big| = 1$. The intensity of $q(x,t)$ is given by $-w(x)$, which shows that solution (61) represents the gray soliton since the profile exhibits a dip under the background but does not drop to zero at the dip center. With $C_0 = -\frac{55}{3}$, $C_1 = -\frac{484}{27}$, $\mu = -4$ and $\sigma = 1$ ($r_1 = \frac{1}{2}$) as an example, we depict the gray-soliton profile via solution (61) in Fig. 7.

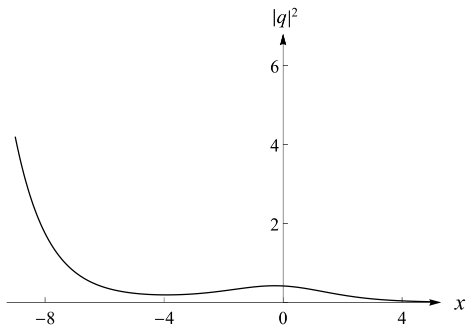

Figure 6: Intensity profile of solution (59) with $C_0 = -\frac{7}{192}$, $C_1 = \frac{5}{3456}$, $\mu = \frac{1}{4}$ and $\sigma = 1$.

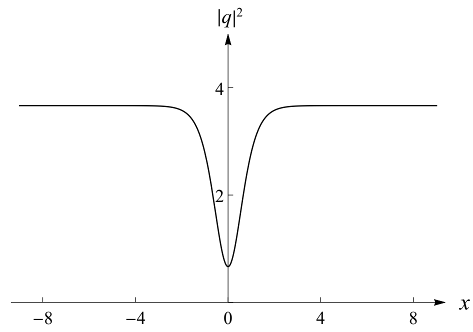

Figure 7: Intensity profile of solution (59) with $C_0 = -\frac{55}{3}$, $C_1 = -\frac{484}{27}$, $\mu = -4$ and $\sigma = 1$.

Case 3: $r_1 = \frac{1}{3}\mu$ $(\mu > 0)$

In this case, we have $C_0 = C_1 = 0$. Then, both solutions (46) and (49) degenerate to the bright-soliton solution:

$$q = i^{\frac{1-\sigma}{2}} \sqrt{2\mu}\,\mathrm{sech}(\sqrt{\mu}\,x)e^{i\mu t} \quad (\mu > 0). \tag{63}$$

In fact, if $r_1 = -\frac{1}{6}\mu\,(\mu < 0)$, one can also obtain the sign-definite $w(x)$ as given in Eq. (35). But remark 1 says that the smooth solution cannot be yielded in such case. Meanwhile, by noticing that

$$\mathrm{sn}(x+K,m) = \frac{\mathrm{cn}(x,m)}{\mathrm{dn}(x,m)}, \quad \mathrm{dn}(x+K,m) = \frac{\sqrt{1-m}}{\mathrm{dn}(x,m)}, \tag{64}$$

we can just derive some trivial results (e.g., 0 or nonzero constant) from the K-shifted Jacobian elliptic-function solutions in section 3.2.3 at the degeneration $r_1 = r_2 > r_3$.

4 Conclusions and discussions

In this paper, with the stationary-solution assumption, we have connected the RTNLS and RSTNLS equations with the standard WE equation, and then have derived their Jacobian elliptic-function and hyperbolic-function solutions. For the RTNLS equation (3), we have obtained the dn-, cn-, sn-, sech- and $\tanh$-function solutions. All those solutions are bounded for $x \in \mathbb{R}$ with the nonsingular conditions, and they contain an arbitrary complex constant x_0. Specially, the tanh-function solution (21) can display both the dark- and antidark-soliton profiles, which depends on the imaginary part of x_0. For the RSTNLS equation (4), we have obtained the general Jacobian elliptic-function solutions, the bounded dn- and cn-function solutions, as well as the K-shifted dn- and sn-function solutions. Those general Jacobian elliptic-function solutions include two cases: the unbounded case ($C_1 > 0$) exhibits an exponential growth as $x \to \infty$ or $-\infty$, while the bounded case ($C_1 < 0$) displays the periodical oscillation but do not drop to 0 at its all minima. At the degeneration $r_1 = r_2 > r_3$, we have found that the hyperbolic-function solutions are exponentially growing at one infinity, or show the gray- and bright-soliton profiles. It should be noted that the $\tanh$-function solution (i.e., the black soliton) is absent for Eq. (4).

On comparing Eqs. (1)–(4), we can draw the following conclusions: (i) The NLS and RSNLS equations, respectively, admit the general bounded and unbounded Jacobian elliptic-function solutions, the RSTNLS equation has both two types of solutions, but the RTNLS equation has none of them. (ii) The NLS, RSNLS and RTNLS equations possess the bounded dn-, cn-, sn-, sech- and $\tanh$-function solutions with the difference lying in their correspondence to the types of nonlinearity, whereas the RSTNLS equation has just the dn-, cn- and sech-function solutions. (iii) An arbitrary constant x_0 (which belongs to $\mathbb{R}$, $i\mathbb{R}$ and $\mathbb{C}$, respectively) is involved in the solutions of the NLS, RSNLS and RTNLS equations, but such a constant is missing for the RSTNLS equation. (iv) The traveling-wave solutions can be obtained from the stationary solutions only for Eqs. (1) and (4). As a matter of fact, the last two results can be seen clearly from the Galilean-invariant transformations of Eqs. (1)–(4):

$$\begin{aligned}
&\text{NLS}: \quad q(x,t) \to \tilde{q}(x+vt+x_0,t)e^{-\frac{ivx}{2}-\frac{iv^2t}{4}} && (v,\, x_0 \in \mathbb{R}),\\
&\text{RSNLS}: \quad q(x,t) \to \tilde{q}(x+ivt+ix_0,t)e^{\frac{vx}{2}+\frac{iv^2t}{4}} && (v, x_0 \in \mathbb{R}),\\
&\text{RTNLS}: \quad q(x,t) \to \tilde{q}(x+x_0,t) && (x_0 \in \mathbb{C}),\\
&\text{RSTNLS}: \quad q(x,t) \to \tilde{q}(x+vt,t)e^{-\frac{ivx}{2}-\frac{iv^2t}{4}} && (v \in \mathbb{C}).
\end{aligned} \tag{65}$$

For the future study on the RTNLS and RSTNLS equations, we mention that the obtained solutions can be used as the seeds to construct the higher-order solutions via the Darboux transformation. Then, one can study the collisions among multiple solitons or multiple Jacobian elliptic-function waves over different nonzero backgrounds [52, 53]. For example, solution (21) with $x_{0I} = \frac{4n+1}{4}\pi$ can yield a new kind of constant-amplitude waves with the nonlinear phase varying with x. Some special attention should be paid to the nonlinear wave dynamics on such constant-amplitude background. In addition, it might be interesting to study the stability problems of those solutions since most of them have not been reported before.

Acknowledgements

This work was partially supported by the National Natural Science Foundation of China (Grant No. 11705284), by the Natural Science Foundation of Beijing Municipality (Grant No. 1212007), by the Science Foundations of China University of Petroleum, Beijing (Grant Nos. 2462020YXZZ004 and 2462020XKJS02), and by the Fundamental Research Funds of the Central Universities (Grant No. 2020MS043).

References

[1] M. J. Ablowitz and P. A. Clarkson, *Solitons, nonlinear evolution equations and inverse scattering* (Cambridge University Press, Cambridge, 1992).

[2] V. E. Zakharov and S. V. Manakov, On the complete integrability of a nonlinear Schrödinger equation, *Theor. Math. Phys.* **19** (1974) 551-559.

[3] M. J. Ablowitz, B. Prinari and A. D. Trubatch, *Discrete and continuous nonlinear Schrödinger systems* (Cambridge University Press, Cambridge, 2004).

[4] M. J. Ablowitz and Z. H. Musslimani, Integrable nonlocal nonlinear Schrödinger equation, *Phys. Rev. Lett.* **110** (2013) 064105.

[5] M. J. Ablowitz and Z. H. Musslimani, Inverse scattering transform for the integrable nonlocal nonlinear Schrödinger equation, *Nonlinearity* **29** (2016) 915-946.

[6] M. J. Ablowitz, X. D. Luo and Z. H. Musslimani, Inverse scattering transform for the nonlocal nonlinear Schrödinger equation with nonzero boundary conditions, *J. Math. Phys.* **59** (2018) 011501.

[7] V. S. Gerdjikov and A. Saxena, Complete integrability of nonlocal nonlinear Schrödinger equation, *J. Math. Phys.* **58** (2017) 013502.

[8] Ya. Rybalko and D. Shepelsky, Long-time asymptotics for the integrable nonlocal nonlinear Schrödinger equation, *J. Math. Phys.* **60** (2019) 031504.

[9] B. Yang and J. K. Yang, Transformations between nonlocal and local integrable equations, *Stud. Appl. Math.* **140** (2018) 178-201.

[10] P. M. Santini, The periodic Cauchy problem for PT-symmetric NLS, I: The first appearance of rogue waves, regular behavior or blow up at finite times, *J. Phys. A* **51** (2018) 495207.

[11] F. Genoud, Instability of an integrable nonlocal NLS, *C. R. Math. Acad. Sci. Paris* **355** (2017) 299-303.

[12] A. K. Sarma, M. A. Miri, Z. H. Musslimani and D. N. Christodoulides, Continuous and discrete Schrödinger systems with parity-time-symmetric nonlinearities, *Phys. Rev. E* **89** (2014) 052918.

[13] A. Khare and A. Saxena, Periodic and hyperbolic soliton solutions of a number of nonlocal nonlinear equations, *J. Math. Phys.* **56** (2015) 032104.

[14] M. Li and T. Xu, Dark and antidark soliton interactions in the nonlocal nonlinear Schrödinger equation with the self-induced parity-time-symmetric potential, *Phys. Rev. E* **91** (2015) 033202.

[15] M. Li, T. Xu and D. X. Meng, Rational solitons in the parity-time-symmetric nonlocal nonlinear Schrödinger model, *J. Phys. Soc. Jpn.* **85** (2016) 124001.

[16] T. Xu, S. Lan, M. Li, L. L. Li and G. W. Zhang, Mixed soliton solutions of the defocusing nonlocal nonlinear Schrödinger equation, *Physica D* **390** (2019) 47-61.

[17] X. Y. Wen, Z. Y. Yan and Y. Q. Yang, Dynamics of higher-order rational solitons for the nonlocal nonlinear Schrödinger equation with the self-induced parity-time-symmetric potential, *Chaos* **26** (2016) 063123.

[18] Y. S. Zhang, D. Q. Qiu, Y. Cheng and J. S. He, Rational solution of the nonlocal nonlinear Schrödinger equation and its application in optics, *Rom. J. Phys.* **62** (2017) 108.

[19] B. F. Feng, X. D. Luo, M. J. Ablowitz and Z. H. Musslimani, General soliton solution to a nonlocal nonlinear Schrödinger equation with zero and nonzero boundary conditions, *Nonlinearity* **31** (2018) 5385-5409.

[20] X. Huang and L. M. Ling, Soliton solutions for the nonlocal nonlinear Schrödinger equation, *Eur. Phys. J. Plus* **131** (2016) 148.

[21] G. Q. Zhang, Z. Y. Yan and Y. Chen, Novel higher-order rational solitons and dynamics of the defocusing integrable nonlocal nonlinear Schrödinger equation via the determinants, *Appl. Math. Lett.* **69** (2017) 113-120.

[22] B. Yang and J. K. Yang, Rogue waves in the nonlocal PT-symmetric nonlinear Schrödinger equation, *Lett. Math. Phys.* **109** (2019) 945-973.

[23] J. K. Yang, General N-solitons and their dynamics in several nonlocal nonlinear Schrödinger equations, *Phys.*

Lett. A **383** (2019) 328-337.

[24] B. Yang and Y. Chen, Dynamics of high-order solitons in the nonlocal nonlinear Schrödinger equations, *Nonlinear Dyn.* **94** (2018) 489-502.

[25] J. Michor and A. L. Sakhnovich, GBDT and algebro-geometric approaches to explicit solutions and wave functions for nonlocal NLS, *J. Phys. A* **52** (2019) 025201.

[26] T. Xu, Y. Chen, M. Li and D. X. Meng, General stationary solutions of the nonlocal nonlinear Schrödinger equation and their relevance to the $\mathcal{PT}$-symmetric system, *Chaos* **29** (2019) 123124.

[27] B. Yang and J. K. Yang, On general rogue waves in the parity-time-symmetric nonlinear Schrödinger equation, *J. Math. Anal. Appl.* **487** (2020) 124023.

[28] W. P. Zhong, Z. P. Yang, M. Belić and W. Y. Zhong, Breather solutions of the nonlocal nonlinear self-focusing Schrödinger equation, *Phys. Lett. A* **395** (2021) 127228.

[29] M. J. Ablowitz and Z. H. Musslimani, Integrable nonlocal nonlinear equations, *Stud. Appl. Math.* **139** (2016) 7-59.

[30] M. J. Ablowitz, B. F. Feng, X. D. Luo and Z. H. Musslimani, Inverse scattering transform for the nonlocal reverse space-time nonlinear Schrödinger equation, *Theor. Math. Phys.* **196** (2018) 1241-1267.

[31] W. X. Ma, Inverse scattering for nonlocal reverse-time nonlinear Schrödinger equations, *Appl. Math. Lett.* **102** (2020) 106161.

[32] B. Yang and Y. Chen, Several reverse-time integrable nonlocal nonlinear equations: Rogue-wave solutions, *Chaos* **28** (2018) 053104.

[33] R. Ye and Y. Zhang, General soliton solutions to a reverse-time nonlocal nonlinear Schrödinger equation, *Stud. Appl. Math.* **10** (2020) 12317.

[34] M. J. Ablowitz, D. J. Kaup, A. C. Newell and H. Segur, Nonlinear-evolution equations of physical significance, *Phys. Rev. Lett.* **31** (1973) 125-127.

[35] D. J. Kaup and A. C. Newell, An exact solution for a derivative nonlinear Schrödinger equation, *J. Math. Phys.* **19** (1978) 798-801.

[36] M. Wadati, K. Konno and Y. Ichikawa, New integrable nonlinear evolution equations, *J. Phys. Soc. Jpn.* **47** (1979) 1698-1700.

[37] M. J. Ablowitz, B. F. Feng, X. D. Luo and Z. H. Musslimani, Reverse space-time nonlocal Sine-Gordon/Sinh-Gordon equations with nonzero boundary conditions, *Stud. Appl. Math.* **141** (2018) 267-307.

[38] M. J. Ablowitz and Z. H. Musslimani, Integrable discrete PT symmetric model, *Phys. Rev. E* **90** (2014) 032912.

[39] A. S. Fokas, Integrable multidimensional versions of the nonlocal nonlinear Schrödinger equation, *Nonlinearity* **29** (2016) 319-324.

[40] Z. Y. Yan, Integrable PT-symmetric local and nonlocal vector nonlinear Schrödinger equations: A unified two-parameter model, *Appl. Math. Lett.* **47** (2015) 61-68.

[41] Z. X. Zhou, Darboux transformations and global solutions for a nonlocal derivative nonlinear Schrödinger equation, *Commun. Nonlinear Sci. Numer. Simulat.* **62** (2018) 480-488.

[42] J. Cen, F. Correa and A. Fring, Integrable nonlocal Hirota equations, *J. Math. Phys.* **60** (2019) 081508.

[43] J. C. Chen and Q. X. Yan, Bright soliton solutions to a nonlocal nonlinear Schrödinger equation of reverse-time type, *Nonlinear Dyn.* **100** (2020) 2807-2816.

[44] S. Y. Lou, Alice-Bob systems, P-T-C symmetry invariant and symmetry breaking soliton solutions, *J. Math. Phys.* **59** (2018) 083507.

[45] S. Y. Lou, Multi-place physics and multi-place nonlocal systems, *Commun. Theor. Phys.* **72** (2020) 057001.

[46] T. A. Gadzhimuradov and A. M. Agalarov, Towards a gauge-equivalent magnetic structure of the nonlocal nonlinear Schrödinger equation, *Phys. Rev. A* **93** (2016) 062124.

[47] M. J. Ablowitz and Z. H. Musslimani, Integrable nonlocal asymptotic reductions of physically significant nonlinear equations, *J. Phys. A* **52** (2019) 15LT02.

[48] T. A. Gadzhimuradov, Envelope solitons in a nonlinear string with mirror nonlocality, *Nonlinear Dyn.* **96** (2019) 1939.

[49] L. D. Carr, C. W. Clark and W. P. Reinhardt, Stationary solutions of the one-dimensional nonlinear Schrödinger equation. I. Case of repulsive nonlinearity, *Phys. Rev. A* **62** (2000) 063610.

[50] L. D. Carr, C. W. Clark and W. P. Reinhardt, Stationary solutions of the one-dimensional nonlinear Schrödinger equation. II. Case of attractive nonlinearity, *Phys. Rev. A* **62** (2000) 063611.

[51] E. T. Whittaker and G. N. Watson, *A course of modern analysis* (Cambridge Press, Cambridge, 1927).

[52] J. B. Chen and D. E. Pelinovsky, Rogue periodic waves of the focusing nonlinear Schrödinger equation, *Proc. R. Soc. A* **474** (2018) 20170814.

[53] X. Gao and H. Q. Zhang, Rogue waves for the Hirota equation on the Jacobi elliptic cn-function background, *Nonlinear Dyn.* **101** (2020) 1159-1168.